Chinese Chemical Letters 33 (2022) 3968–3972

Contents lists available at ScienceDirect

Chinese Chemical Letters

journal homepage: www.elsevier.com/locate/cclet

# Self-assembly of reverse micelle nanoreactors by zwitterionic polyoxometalate-based surfactants for high selective production of $\beta$–hydroxyl peroxides

Guicong Hu, Wen Chang, Sai An, Bo Qi*, Yu-Fei Song*

*State Key Laboratory of Chemical Resource Engineering, Beijing University of Chemical Technology, Beijing 100029, China*

ARTICLE INFO

*Article history:*
Received 6 October 2021
Revised 27 October 2021
Accepted 1 November 2021
Available online 7 November 2021

*Keywords:*
Polyoxometalate
Self-assembly
Peroxide
Catalysis
Zwitterionic surfactant

ABSTRACT

Surfactants with polyoxometalates (POMs) as polar head groups have shown fascinating self-assembly behaviors and various functional applications. However, self-assembly them into reverse micelles is still challenging owing to the large molecular size and intermolecular strong electrostatic repulsions of POM heads. In this work, a zwitterionic POM-based surfactant was synthesized by covalently grafting two cationic long alkyl tails onto the lacunary site of $[PW_{11}O_{39}]^{7-}$. With decreased electrostatic repulsions and increased hydrophobic effect, the POM-based reverse micelles with an average diameter of 5 nm were obtained. Interestingly, when these reverse micelles were applied for catalyzing the oxidation of styrene, an unprecedented $\beta$–hydroxyl peroxide compound of 2–hydroxyl-2-phenylethan-1–*tert*-butylperoxide was produced in high selectivity of 95.2%. In comparison, the cetyltrimethylammonium electrostatically encapsulated POMs mainly generated the epoxides or 1,2-diols. A free radical mechanism was proposed for the oxidation reaction catalyzed by the zwitterionic POM surfactants.



Reverse micelles (RMs) are nanometer-sized assemblies of surfactants organized around a core of water molecules within a bulk nonpolar solvent. RMs have wide applications in the extraction of protein, enzymatic reaction, nanomaterial synthesis, drug delivery, and catalysis [1,2]. With loading catalysts into the special confined water core, RMs have shown many unique catalytic behaviors [3]. Several reports indicated that some catalysts, like enzymes or metal nanoparticles, appeared to behave differently when confined in RMs than in bulk solution, because of the conformational changes of reactants, the local concentrated of catalysts and substrates, and the confined water that may lead to an altered hydration state of the active sites [4–6]. With the development of RMs, integrating the catalytic activity and amphiphilic properties into one surfactant molecule is an emerging field, which offers more possibilities for novel catalytic systems with excellent performance, high stability, or even new reactions [7]. Recently, the multifunctional polyoxometalates, with variable negative charges and notable redox properties, were facilitated as the polar head groups of anionic surfactants. These compounds have shown unusual self-assembly behaviors, interesting photochemical properties, and excellent catalytic activity [8–10].

However, the self-assembly of RMs by POM-based surfactants is extremely challenging, and their further catalytic applications are rarely explored. As the nanoscale size of the POM head group results in a large hydrophilic area, the packing parameters (*P*) of POM-based surfactants are often less than 1, which favors the formation of micelles, vesicles, or emulsions. Whereas, a larger *P* is essential for the assembly of RMs. In addition, the multiple negative charges of the POM clusters lead to strong electrostatic repulsions, which prevent the POMs from approaching each other, thus hamper the self-assembly process of RMs. There have been studies for increasing the *P*, such as fabricating two long alkyl tails modified Keggin-type POMs or using Anderson-type POMs as a smaller head [11–13]. However, only liquid crystals or reverse-vesicular structures were obtained. Beyond the anionic POM-based surfactant, a new type of the surfactant structure is crucial to be synthesized for self-assembly into the RMs. What is more, it is also an opportunity to develop the novel catalytic behaviors of POMs when they are concentrated and confined in the core of RMs.

In this work, we prepared a series of novel POM-based zwitterionic surfactant molecules that two cationic quaternary amine long chains were covalently grafted on the Keggin POM anion *via* Si—O—W bonds. For the first time, the POM-based reverse micelle

* Corresponding authors.
*E-mail addresses:* bqi@mail.buct.edu.cn (B. Qi), songyf@mail.buct.edu.cn (Y.-F. Song).

https://doi.org/10.1016/j.cclet.2021.11.006
1001-8417/

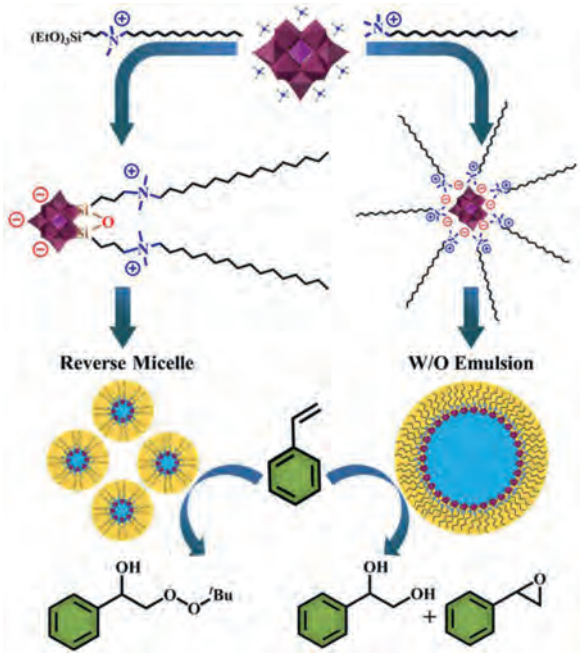


**Scheme 1.** Illustration for the self-assembly of reverse micelles by zwitterionic POM-based surfactant Na−$PW_{11}$−$NC_{16}$ which facilitate the oxidation of styrene to $\beta$–hydroxy peroxide (left), and the self-assembly of W/O emulsions by electrostatically bonded POM-cationic surfactant salt CTA + $PW_{11}$ which favor the epoxides and 1,2-diols products (right).

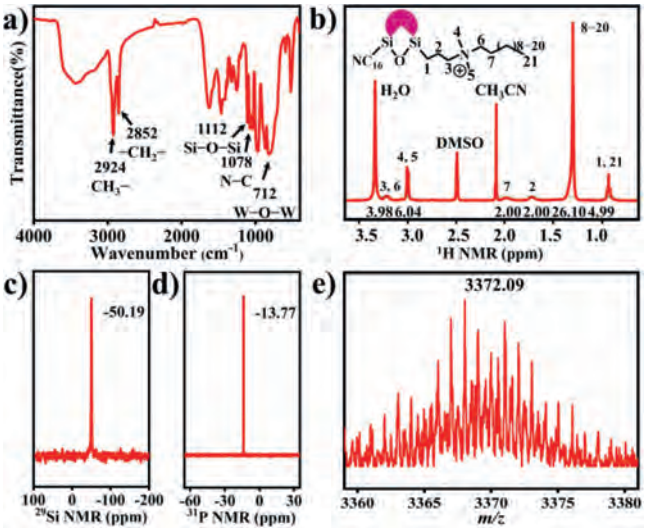


**Fig. 1.** The characterizations of Na−$PW_{11}$−$NC_{16}$ with a formula of $Na\{PW_{11}O_{39}[SiO_{0.5}(CH_2)_3N(CH_3)_2C_{16}H_{33}]_2\}$ by (a) FT-IR spectrum, (b) $^1$H NMR spectrum, (c) solid-state $^{29}$Si NMR spectrum, (d) $^{31}$P NMR spectrum and (e) ESI-MS spectrum.

systems were successfully fabricated through the self-assembly of zwitterionic surfactants. On the contrary, the cationic surfactants encapsulated POMs were assembled into the water in oil (W/O) emulsion systems under the same condition. When evaluating their catalytic behaviors in the oxidation of styrene, the reverse micelles highly selective produced a $\beta$–hydroxyl peroxide compound while the emulsions mainly generated the epoxides and 1,2-diols (Scheme 1).

Initially, a series of cationic organosilane ligands $(EtO)_3Si(CH_2)_3N^+(CH_3)_2C_nH_{2n+1}$ were synthesized by a nucleophilic substitution reaction of (3-iodopropyl)triethoxysilane with long-chain *N,N*-dimethylalkylamines $(CH_3)_2N(CH_2)_{n-1}CH_3$ ($n$ = 8, 12, 16) [26]. The ligands were characterized and denoted as the abbreviation of $NC_n$ (Figs. S1−S10 in Supporting information). It has been reported that the neutral organosilane species can be covalently inserted into the pocket of the lacunary Keggin anion in $H_2O/CH_3CN$ mixed solution [14,15]. While for the modification of cationic ligands, unfavorable electrostatically interacted POM salts may be formed and further precipitated out due to their low solubility in water. Therefore, an excess tetramethylammonium (TMA) salt was added into the reaction solution for competing with the cation-anion interaction between ligands and POMs. Besides, a high portion of $CH_3CN$ was used as a good solvent for finely dispersing the reactants. With the modified preparation methods, the desired products $TMA[PW_{11}O_{39}(SiO_{0.5}(CH_2)_3N(CH_3)_2C_nH_{2n+1}]_2)]$ (TMA−$PW_{11}$−$NC_n$) were obtained. Subsequently, the counterions were exchanged to sodium ions for increasing the amphiphilicity of POM-based surfactants.

The resulting POM surfactants were characterized by FT-IR, $^1$H NMR, $^{13}$C NMR, $^{29}$Si NMR, $^{31}$P NMR and electron spray ionization mass spectra (ESI-MS). The characterization results of representative sample Na−$PW_{11}$−$NC_{16}$ were shown in Fig. 1. In FT−IR spectroscopy of Na−$PW_{11}$−$NC_{16}$ (Fig. 1a and Fig. S24 in Supporting information), peaks of the alkyl chains (2924, 2852, 1463, 1078 $cm^{-1}$) and the POM cluster (1038, 967, 900, 871, 822, 712 $cm^{-1}$) were visible. The peaks of 1112 and 1078 $cm^{-1}$ represented the vibrations of the Si−O−Si bond and the stretching vibrations of the C−N bonds for quaternary amine cations, which inferred that the cationic ligands were modified onto the POM cluster. It should be noted that the Si−OEt groups were crucial to link the organic ligands with $PW_{11}$, while they were highly sensitive to the water, which may result in hydrolysis and self-polymerization. In $^1$H NMR spectra (Fig. S25 in Supporting information), signals of the quartet at 3.83 ppm and the triplet at 1.24 ppm (stars signs) suggested that the Si−OEt groups existed in $NC_{16}$ ligands. After the covalent modification, these signals were disappeared, indicating the replacement of Si−OEt to Si−O−Si or Si−O−W groups in TMA−$PW_{11}$−$NC_{16}$ samples. For TMA−$PW_{11}$−$NC_{16}$, the intensity ratio of the protons of *N,N*-dimethyl in two ligand chains (3.04, 3.06 ppm, 12H, square) and methyl protons of $TMA^+$ (3.11 ppm, 12H, triangle) was around 1 suggesting that the whole polar head had one negative charge, which was in agreement with the theoretical net charge. The complete counterion exchange from $TMA^+$ to $Na^+$ was proven by the absence of the signals of $TMA^+$ in Na−$PW_{11}$−$NC_{16}$ (Fig. 1b). The modification of the POM cluster can also be confirmed by the unique signals of −13.77 ppm in $^{31}$P NMR and −51.7 ppm in $^{29}$Si NMR spectra, which were attributed to the structure of two organosilicate embedded to the lacunary site of the $PW_{11}$ cluster (Figs. 1c and d). Moreover, only one signal exists in both spectra indicated that the product was pure. From the ESI-MS spectrum (Fig. 1e), the molecule mass of Na−$PW_{11}$−$NC_{16}$ with a formula of $Na\{PW_{11}O_{39}[SiO_{0.5}(CH_2)_3N(CH_3)_2C_{16}H_{33}]_2\}$ was determined as 3372.09 *m/z*, which was consistent with theory. Furthermore, from the analysis of the TG curve (Fig. S43 in Supporting information), the ligand chains were degrade from 372.6 °C to 506.5 °C and the POM head was retained even the temperature higher than 700 °C, confirming the considerable thermal stability of Na−$PW_{11}$−$NC_{16}$. The co-existence of anionic and cationic centers in Na−$PW_{11}$−$NC_{16}$ was proven by the dye extraction experiments. With adding one drop of the aqueous solution of cationic dye methylene blue into the chloroform solution of Na−$PW_{11}$−$NC_{16}$, the blue color was extracted to the nonpolar phase. The same phenomenon was also observed when the dye was anionic methyl orange. These phenomena suggested that both the cationic dye and anionic dye could be captured by the zwitterionic center of the Na−$PW_{11}$−$NC_{16}$ surfactant (Fig. S29 in Supporting information). Based on the above characterizations, the struc-

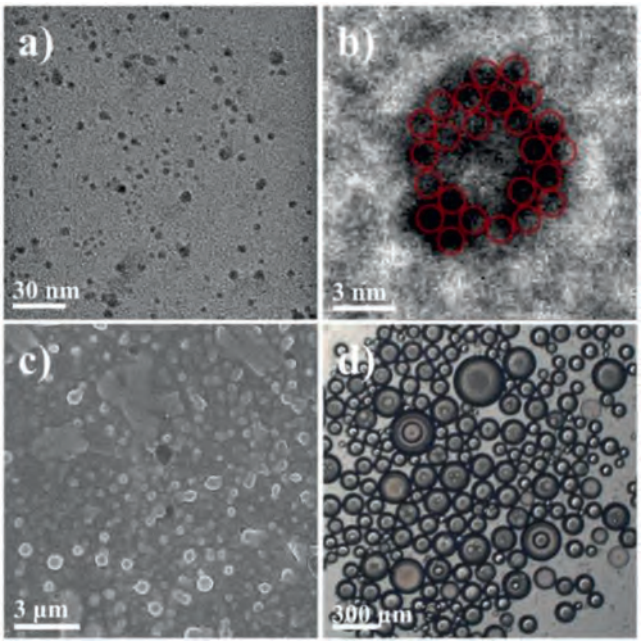


**Fig. 2.** (a) TEM image of the Na−$PW_{11}$−$NC_{16}$ assembled reverse micelles with an average diameter around 5 nm. (b) Magnified HR-TEM image of one POM-based reverse micelle showed the aggregation of POM clusters as 1 nm dark spots. (c) SEM image of the emulsions assembled by Na-$PW_{11}$-$NC_{12}$. (d) Optical microscope image of W/O emulsions assembled by CTA + $PW_{11}$.

ture of the surfactant Na−$PW_{11}$−$NC_n$ could be proposed, in which the nonpolar tail groups were two alkyl long chains and the polar head group was the covalently linked POM anion and quaternary amine cations. For comparison, the cationic surfactants encapsulated POM salts were prepared by directly mixing the $K_7PW_{11}O_{39}$ with surfactants like cetyltrimethylammonium bromide (CTAB) in an aqueous solution and collecting the resulted salt precipitates (CTA + $PW_{11}$).

After determining the structures, the self-assembly behaviors of the Na−$PW_{11}$−$NC_{16}$ zwitterionic surfactants were developed. It showed that the hydrophilicity of the POM group was significantly decreased after grafting the organic ligands, which was still not improved even after the counterions were exchanged to $Na^+$. Solubility experiments were conducted by preparing 1 mg/mL Na−$PW_{11}$−$NC_{16}$ in different solvents. The results suggested that the Na−$PW_{11}$−$NC_{16}$ was highly soluble in DMF, DMSO, acetone, and acetonitrile, while less soluble in water, methanol, toluene, and chloroform. To construct the reverse micelle systems, the Na−$PW_{11}$−$NC_{16}$ (10 mg) were firstly dissolved in 0.2 mL DMF, and then the above solution was slowly titrated into the chloroform (10 mL) with stirring. A colorless transparent solution was formed after adding 1 mL *tert*–butyl hydroperoxide (TBHP) 70% aqueous solution. Transmission electron microscopy (TEM) revealed that the assemblies had a spherical appearance in a size range of 3–8 nm (Fig. 2a, Figs. S30 and S31 in Supporting information). The mentioned value fits well to the diameter expected for a reverse micellar aggregate constructed from zwitterionic POM surfactants. Taking advantage of the characteristic of high electronegativity and the well-fitted 1 nm molecular size of Keggin clusters, the $PW_{11}$ head groups could be easily observed in these small particles as 1 nm dark spots in HR-TEM images (Fig. 2b). Thus, it was believed that the Na−$PW_{11}$−$NC_{16}$ zwitterionic surfactants were self-assembled into the reverse micelles, and their $PW_{11}$ head groups were compactly located into the nano-sized core of RMs.

Then, the self-assembly mechanism of RMs was discussed. The TBHP in solution seemed to play an essential role in the assembly process. Instead of 70% TBHP aqueous solution, 300 μL water was added to trigger the assembly. A cloudier solution was obtained, and some water drops were observed on the inner surface of the glass vial. Thus, it was speculated that the TBHP served as a co-surfactant inserting among the intermolecular of Na−$PW_{11}$−$NC_{16}$ to strengthen the stability of the interface and promote the solubilization of water. The conformation of TBHP in RMs was proposed that *tert*–butyl group located in the nonpolar area and hydroperoxide group pointed to the core water area. The corresponding experiments with the CTA + $PW_{11}$ (Fig. 2d and Fig. S28 in Supporting information) in the same conditions showed the large size W/O emulsions with a non-transparent milky white appearance. The results suggested that the electrostatically bonded CTA + $PW_{11}$ was incapable of self-assembly into the RMs and the covalent modified zwitterionic head groups contributed to the RMs' formation. In fact, the zwitterionic properties of surfactants could significantly decrease the electrostatic repulsions among the head groups, which favored the compact arrangement of head groups and thus forming the thermodynamically stable RMs. Moreover, considering the assembly was driven by the balance between electrostatic interaction and hydrophobic effect, influence from the chain length of POM surfactant was investigated. The results showed that neither Na−$PW_{11}$−$NC_{12}$ nor Na−$PW_{11}$−$NC_8$ could assemble into the RMs. Instead, emulsions with ~0.5 μm size for Na−$PW_{11}$−$NC_{12}$ (Fig. 2c) and large amounts of precipitates for Na−$PW_{11}$−$NC_8$ (Fig. S27 in Supporting information) occurred. It was suggested that the shorter chain length had less solubility in chloroform, and the corresponding lower strength of hydrophobic interaction was insufficient to overcome the electrostatic repulsions. Therefore, the self-assembly of RMs was synergistically driven by the decreased electrostatic repulsions and the increased hydrophobic interaction, as well as the co-surfactant effect from TBHP.

Recently, the synthesis of $\beta$–hydroxy peroxides by direct oxidation of olefins has gained great attention for the preparation of active 1,2,4-trioxane units, which are present in the anti-malarial drugs artemisinin (Qinghaosu) and play a crucial role in the drug's mechanism of action [16]. The POMs are widely used as catalysts in the oxidation of olefins due to their notable redox properties, strong persistence against oxidants, and environmental compatibility [17-19,23-25]. In most cases, the oxidation products are epoxides or 1,2-diols, the peroxy-containing products are rarely reported.

Taking the opportunity of POMs self-assembly into the novel RMs, an unprecedented product 2–hydroxyl-2-phenylethan-1–*tert*-butylperoxide was obtained by applying the RMs as nanoreactors with styrene as substrate. The structure of the product was determined by the $^1$H NMR, $^{13}$C NMR and ESI-MS spectra. In the $^1$H NMR spectrum (Fig. S32 in Supporting information), three pairs of *dd* characteristic peaks at 5.34, 4.25 and 4.16 ppm with an integration ratio of 1:1:1 were corresponding to the protons of ethyl groups. After comparing with the characteristic protons in the same position of styrene oxide (3.83, 2.96, 2.71 ppm) and 1-phenylethane-1,2-diol (4.88, 4.13, 3.88 ppm), we confirmed that the C=C bond of styrene was substituted by two functional groups (Fig. S36 in Supporting information). Combined with the fact that the *t*Bu peak (s, 1.28 ppm, 9H) in the $^1$H NMR spectrum and the mass peak at 249.06 (M + $K^+$) in the ESI−MS spectrum (Fig. S33 in Supporting information), it was suggested that the substituted functional groups were hydroxyl and *tert*–butyl peroxy, separately. For the structure of isomers, it was hard to determine whether the peroxy group was added to the $\alpha$ or $\beta$ position of styrene only by $^1$H NMR results, because the shielding effect from the peroxy and hydroxyl group on ortho protons were almost the same. Therefore, the $^{13}$C NMR spectrum (Fig. S35 in Supporting information) was acquired for the carbon atoms that were more sensitive to

**Table 1**
Catalysts control experiments of styrene oxidation reaction[a].

| Entry | Catalysts | Yield (%) [b] | | | Sel. (%) [b] | |
|---|---|---|---|---|---|---|
| | | A | B | C | A | B + C |
| 1 | $Na-PW_{11}-NC_{16}$ | 43.1 | 2.2 | 0 | 95.2 | 4.8 |
| 2 | $NC_{16}$ | trace | 0 | 0 | –– | –– |
| 3 | $PW_{11}$ | 14.3 | 2.9 | 1.9 | 69.6 | 30.4 |
| 4 | $HNC_{16}$ + $PW_{11}$ | 5.7 | 17.2 | 0 | 24.9 | 75.1 |
| 5 | CTA + $PW_{11}$ | 6.2 | 18.1 | 3.2 | 22.9 | 77.1 |

[a] Reaction conditions: Styrene (1 mmol), TBHP (70% aqueous solution, 6 mmol), DMF (0.2 mL), $CHCl_3$ (10 mL).
[b] Yield and selectivity were determined by using $^1H$ NMR analysis with an internal standard.

the connected groups. A styrene difunctional compound (1-(*tert*–butylperoxy)–3,3,3-trifluoropropyl)benzene, in which the peak of the *t*BuOO group linked carbon atom appeared at 80.83 ppm, was selected as the isomer standard [20]. In the $^{13}C$ NMR spectrum (Fig. S34 in Supporting information) of the obtained product, peaks at 76.65 ppm and 81.09 ppm were attributed to the carbons at $\alpha$ and $\beta$, respectively. Thus, the *t*BuOO group was located at the $\beta$ position, the OH group was linked with the $\alpha$ position of phenylethane.

Then, the reaction conditions, including solvents, temperature, and equivalents of reactant, were optimized, and the peroxide product was obtained with 43.1% yield and 95.2% selectivity (Tables S1–S3 in Supporting information). Catalysts control experiments were carried out to illustrate the critical role of each component on the peroxide reaction. As shown in Table 1 (entries 1 and 2), the reaction could be scarcely possible initiated in the absence of $PW_{11}$, indicating the active catalytic sites were $PW_{11}$. As for the $K_7PW_{11}O_{39}$, the clusters were partially dissolved in the polar solvents while most residues remained as solid precipitates. The catalytic result showed a decreased peroxide yield (14.3%) and selectivity (69.6%), which may be due to the poor accessibility of styrene to the active sites (Table 1, entry 3). In addition, the physical mixture of $PW_{11}$ and protonated $NC_{16}$ ligands showed a significantly decreased peroxide yield, and the styrene was mainly transformed into epoxides and 1,2-diols with 75.1% selectivity. When the CTA + $PW_{11}$ salts were applied as catalysts, the epoxides and 1,2-diols were also generated in high selectivity of 77.1%. From the perspective of assembly systems, the surfactants encapsulated POM catalysts formed emulsion systems, in which the POM clusters were highly hydrated and contacted with a relative bulk water environment. On the contrary, POMs in the confined water core of RMs had less hydration states which might be favorable to the $\beta$–hydroxyl peroxide transformation. Moreover, there was no change in the FT-IR and $^{31}P$ NMR spectrum (Figs. S41 and S42 in Supporting information) of the $Na-PW_{11}-NC_{16}$ after the reaction, which confirmed that the structure was not affected by the high concentration of TBHP. Furthermore, the scope of substrates was also expanded and the corresponding peroxide products were detected (Table S4 in Supporting information).

To investigate the mechanism of this peroxide reaction, styrene oxide was used as a substrate in the same reaction conditions. The catalytic results showed that no peroxides were produced. Thus, the possibility can be ruled out that styrene was firstly oxidized to styrene oxide then ring open by the TBHP to the $\beta$–hydroxy peroxide product. Subsequently, 2,2,6,6-*tetra*-methyl-1-piperidinyloxy (TEMPO) was employed in the reaction system as a radical scavenger [21]. When adding 6 equivalents of TEMPO, the reaction was completely inhibited without any peroxide products. In addition, when adding a hydroxyl radical scavenger KBr [22], a 1,2–*tert*-butylperoxy-phenylethane was obtained (Figs. S35 and S36). Based on the above results, a free radical pathway was proposed (Fig. S39 in Supporting information). The distinct oxidation pathway may be due to the oxidation state variation of POMs after the organic modification. X-ray photoelectron spectroscopy (XPS) was performed to support the hypothesis. W 4f spectra (Fig. S26 in Supporting information) showed W $4f_{5/2}$ (37.7 eV) and W $4f_{7/2}$ (35.5 eV) of $PW_{11}$, attributing to $W^{6+}$. As expected, the binding energy of W (36.2 and 38.4 eV) in $Na-PW_{11}-NC_{16}$ shifted to a higher energy than that in $PW_{11}$. The results indicated that the electron structure of W was affected by cationic quaternary amine long chains leading to a higher oxidation state of W in the $Na-PW_{11}-NC_{16}$.

In summary, a new type of zwitterionic POM surfactant was prepared by covalently modifying two cationic long alkyl chains onto the mono-lacunary site of $[PW_{11}O_{39}]^{7-}$. Under the cooperation with co-surfactant TBHP, the $Na-PW_{11}-NC_{16}$ could self-assemble into the challenging POM-based reverse micelles with diameters around 5 nm. The mechanism studies demonstrated that the self-assembly was synergistically driven by the decreased electrostatic repulsions among zwitterionic head groups and the increased hydrophobic effect from long alkyl chains. Furthermore, by applying the reverse micelles into the oxidation of styrene, a new compound, 2–hydroxyl-2-phenylethan-1–*tert*-butylperoxide was obtained with 95.2% selectivity. On the contrary, the W/O emulsion systems, which were assembled by the cationic surfactants encapsulated $PW_{11}$, generated epoxides and 1,2-diols with high selectivity of 77.1%. We hope this work will facilitate the further development of POM-based supramolecular assemblies and expand the scope of catalytic applications in fields of new reactions and high value-added peroxide products.

## Declaration of competing interest

The authors declare that they have no known competing financial interests or personal relationships that could have appeared to influence the work reported in this paper.

## Acknowledgments

This work was supported by the Beijing Natural Science Foundation (No. 2202039), the National Natural Science Foundation of China. (Nos. 22178019, 22101017, U1707603, 21625101, 21521005, 21808011), the National Key Research and Development Program of China (No. 2017YFB0307303) and the Fundamental Research Funds for the Central Universities (Nos. XK1802–6, XK1803–05, XK1902, 12060093063).

## Supplementary materials

Supplementary material associated with this article can be found, in the online version, at doi:10.1016/j.cclet.2021.11.006.

## References

[1] F. Zaera, Chem. Soc. Rev. 42 (2013) 2746–2762.
[2] E.P. Melo, M.R. Aires-Barros, J.M.S. Cabral, Biotechnol. Annu. Rev. 7 (2001) 87–129.
[3] A. Küchler, M. Yoshimoto, S. Luginbühl, et al., Nat. Nanotech. 11 (2016) 409–420.
[4] F. Moyano, R.D. Falcone, J.C. Mejuto, et al., Chem. Eur. J. 16 (2010) 8887–8893.
[5] M. Moniruzzaman, N. Kamiya, M. Goto, et al., Langmuir 25 (2009) 977–982.
[6] Y. Qian, W. Wen, P.A. Adcock, et al., J. Phys. Chem. C 112 (2008) 1146–1157.
[7] S. Polarz, S. Landsmann, A. Klaiber, Angew. Chem. Int. Ed. 53 (2014) 946–954.
[8] P. Yin, J. Wang, Z. Xiao, et al., Chem. Eur. J. 18 (2012) 9174–9178.
[9] H.K. Liu, L.J. Ren, H. Wu, et al., J. Am. Chem. Soc. 141 (2019) 831–839.
[10] J. Xu, X. Li, J. Li, et al., Angew. Chem. Int. Ed. 56 (2017) 8731–8735.
[11] S. Landsmann, C. Lizandara–Pueyo, S. Polarz, J. Am. Chem. Soc. 132 (2010) 5315–5321.
[12] J. Zhang, Y.F. Song, L. Cronin, et al., Chem. Eur. J. 16 (2010) 11320–11324.
[13] C.G. Lin, W. Chen, S. Omwoma, et al., J. Mater. Chem. C 3 (2015) 15–18.
[14] G. Izzet, B. Abécassis, D. Brouri, et al., J. Am. Chem. Soc. 138 (2016) 5093–5099.
[15] A. Proust, B. Matt, R. Villanneau, et al., Chem. Soc. Rev. 41 (2012) 7605–7622.

[16] D. Louvel, T.D.D. Miguel, N.D. Vu, et al., Eur. J. Org. Chem. (2021) 2990–3014.
[17] S.S. Wang, G.Y. Yang, Chem. Rev. 115 (2015) 4893–4962.
[18] G. Yang, Y. Liu, K. Li, et al., Chin. Chem. Lett. 31 (2020) 3233–3236.
[19] W. Chang, B. Qi, Y.F. Song, ACS Appl. Mater. Interfaces 12 (2020) 36389–36397.
[20] B. Qi, T. Zhang, M. Li, et al., Catal. Sci. Technol. 7 (2017) 5872–5881.
[21] Y. Chen, Y. Ma, L. Li, et al., Org. Lett. 21 (2019) 1480–1483.
[22] R.R. Ozer, J.L. Ferry, J. Phys. Chem. B 104 (2000) 9444–9448.
[23] G. Yang, X. Zhang, Y. Liu, et al., Inorg. Chem. Front. 8 (2021) 4650–4656.
[24] G. Yang, K. Li, X. Lin, et al., Chin. J. Chem. 39 (2021) 3017–3022.
[25] G. Yang, X. Xie, M. Cheng, et al., Chin. Chem. Lett. 33 (2022) 1483–1487.
[26] M. Zhao, X. Zhu, Y. Li, et al., Tungsten 4 (2022) 121–129.